Temperature enhanced succinate production concurrent with increased central metabolism turnover in the cyanobacterium Synechocystis sp. PCC 6803

Hasunuma, Tomohisa

Matsuda, Mami

Kato, Yuichi

John Vavricka, Christopher

Kondo, Akihiko

(Citation)
Metabolic Engineering,48:109-120

(Issue Date)
2018-07

(Resource Type)
journal article

(Version)
Accepted Manuscript

Temperature enhanced succinate production concurrent with increased central metabolism turnover in the cyanobacterium *Synechocystis* sp. PCC 6803

Tomohisa Hasunuma[a]*, Mami Matsuda[a], Yuichi Kato[a], Christopher John Vavricka[a] and Akihiko Kondo[a,b]

[a] Graduate School of Science, Innovation and Technology, Kobe University, 1-1 Rokkodai, Nada, Kobe 657-8501, Japan

[b] Biomass Engineering Program, RIKEN, 1-7-22 Suehiro, Tsurumi, Yokohama, Kanagawa 230-0045, Japan

*Corresponding author: Tomohisa Hasunuma

Graduate School of Science, Technology and Innovation, Kobe University, 1-1 Rokkodai, Nada, Kobe 657-8501, Japan

Tel: +81-78-803-6356; Fax: +81-78-803-6192

E-mail: hasunuma@port.kobe-u.ac.jp

ABSTRACT

Succinate is a versatile petrochemical compound that can be produced by microorganisms, often from carbohydrate based carbon sources. Phototrophic cyanobacteria including *Synechocystis* sp. PCC 6803 can more efficiently produce organic acids such as succinate without sugar supplementation, via photosynthetic production of glycogen followed by glycogen utilization, typically under dark conditions. In this study, *Synechocystis* 6803 bioproduction of organic acids under dark anoxic conditions was found to increase with elevation of temperature from 30°C to 37°C. The further enhancement of succinate bioproduction by overexpression of the rate limiting enzyme phosphoenolpyruvate carboxylase resulted in improved glycogen utilization. To gain more insight into the mechanisms underlying the increased organic acid output, a novel temperature dependent metabolomics analysis was performed. Adenylate energy charge was found to decrease along with elevating temperature, while central metabolites glucose 6-phosphate, fructose 6-phosphate, fructose 1,6-bisphosphate, glycerol 3-phosphate, malate, fumarate and succinate increased. Temperature dependent ^{13}C-labeling metabolomics analysis further revealed a glycolysis to TCA bottleneck, which could be overcome by addition of CO_2, leading to even higher organic acid production. Optimization of initial cell concentration to 25 g-dry cell weight/L, in combination with 100 mM $NaHCO_3$ supplementation, afforded a succinate titer of more than 1.8 g/L, the highest reported autotrophic succinate titer. Succinate titers remained high after additional knockout of *ackA*, resulting in the highest reported autotrophic D-lactate titer as well. The optimization of *Synechocystis* 6803 organic

acid production therefore holds significant promise for CO_2 capture and utilization.

Key words:

Autofermentation; Cyanobacteria; Lactate; Metabolomics; Succinate; *Synechocystis*; Temperature

1. Introduction

The rapid development of the petrochemical industry in the 20th century has created a mass consumption and disposal social structure, leading to the over-generation of greenhouse gasses including carbon dioxide (CO_2) and global climate change. In order to address these problems and help build a sustainable low-carbon future society, it is necessary to develop technologies to biologically produce fuels and commodity chemicals from renewable biomass. Recently, non-food-based lignocellulosic biomass that exists abundantly on land has attracted attention as a renewable feedstock for microbial fermentation to produce a wide variety of chemicals. However, recalcitrant structures of lignocellulosic biomass make it difficult to generate fermentable sugars from component cellulose and hemicellulose with high yield.

Photosynthetic algae directly convert CO_2 to useful substances including lipid, starch, glycogen, pigments and organic acids (Aikawa et al., 2013; Dismukes et al., 2008; Hasunuma et al., 2016, Ho et al., 2017; Wijffels et al., 2013), which can be utilized to avoid the use of more expensive sugars as well as complicated plant-biomass decomposition processes. Furthermore, algae cultivation does not require agricultural resources such as farmland or fresh water (Iijima et al., 2015).

The unicellular cyanobacterium *Synechocystis* sp. PCC 6803 (hereafter *Synechocystis* 6803) is the first algae to be genome decoded (Kaneko et al., 1996). Along with the development of genetic engineering tools, *Synechocystis* 6803 metabolic pathways have been successfully modified to enhance photosynthetic activity and to produce alcohols, diols, hydrocarbons, organic acids and other

77 valuable chemicals (Angermayr et al., 2015; Formighieri et al., 2015; Hasunuma et
78 al., 2014; Lai and Lan 2015; Lan and Wei, 2016; Wang et al., 2016).

79 *Synechocystis* 6803 inherently produces organic acids including D-lactate
80 and succinate by catabolism of the primary storage polysaccharide glycogen, which
81 accumulates during photosynthesis (Hasunuma et al., 2016). As carbon sources
82 such as sugars and glycerol are not necessary, this type of catabolism is referred to
83 as autofermentation (McNeely et al., 2010). Lactate typically serves as a building
84 block for the synthesis of a bio-based plastic, polylactic acid (PLA). Notably,
85 stereocomplex-type PLA composed of L- and D-lactate is promising due to a high
86 melting point (ca. 230°C) (Ikeda et al., 1987). The current industrial biological
87 production of D-lactate (Wee et al., 2006) remains to be established and is
88 therefore considered to be more important than that of L-lactate.

89 Succinate is also an important raw material of poly(butylene succinate),
90 polyurethanes and other green sustainable plastics (Choi et al., 2015; Delhomme et
91 al., 2009). Various chemicals produced in the current petrochemical industry
92 including adipic acid, 1,4-butanediol, γ-butyrolactone, *N*-methylpyrrolidone and
93 tetrahydrofuran can be produced from succinate as well (Akhtar et al., 2014).

94 The metabolic pathways of autofermenting cyanobacteria are not well
95 characterized as of yet. Recently, dynamic metabolomics using ^{13}C labeling has
96 clarified that succinate is biosynthesized from glycogen via glycolysis, the
97 anaplerotic pathway and reductive TCA cycle in *Synechocystis* 6803 under dark
98 anoxic conditions (Hasunuma et al., 2016). However, optimal culture environments
99 to maximize production of succinate have not yet been determined.

100 Temperature is an important control element in the fermentation process
101 to efficiently produce target molecules (Gourdon and Lindley, 1999; Shin et al.,
102 2007). Yet, the influence of temperature regulation on the total metabolic system of
103 a microorganism has not been reported to our knowledge (Yurkovich et al., 2017).
104 The optimal growth temperature of *Synechocystis* 6803 is 30-32°C (Tasaka
105 et al., 1996). In the present study of *Synechocystis* 6803, elevated temperatures
106 were found to increase production of organic acids including D-lactate and
107 succinate. The highest production of D-lactate and succinate was observed at 37°C
108 to 40°C.
109 So far, the optimal temperature range of various enzymes involved in
110 central metabolism has been investigated *in vitro*. However, *in vivo* metabolic
111 turnover, which is dependent on activated-enzyme level and intracellular
112 environment such as molecular crowding, differs from the *in vitro* data. Thus, in the
113 present study, influence of elevated temperature on central metabolism was
114 systematically analyzed using a dynamic metabolome analysis developed by
115 combining *in vivo* ^{13}C labeling, metabolomics and mass distribution determination.
116 This comprehensive approach afforded direct observation of *in vivo* kinetics and
117 carbon distribution in *Synechocystis* 6803. Elevating temperature to 37°C was
118 found to enhance organic acid bioproduction in both wild type and
119 phosphoenolpyruvate carboxylase (PEPC) overexpressing *Synechocystis* 6803.
120 Furthermore, a glycolysis to TCA bottleneck was discovered and alleviated via
121 addition of CO_2, which significantly increased succinate titers to 1,802 mg/L.
122

2. Materials and Methods

2.1. Strains and culture conditions

A recombinant *Synechocystis* 6803 strain, referred to as Ppc-ox, overexpresses the endogenous PEPC gene (*ppc*, *sll0920*) under the control of the *trc* promoter. The Ppc-ox strain was constructed from a wild type GT strain (Williams, 1988) as described previously (Hasunuma et al., 2016). Recombinant and GT strains were cultivated in BG11 medium (Rippka et al., 1979) with and without 50 mg/L kanamycin, respectively, under photoautotrophic conditions. Cell density was observed by optical density at 750 nm (OD_{750}). Sampling volumes were determined based on g-dry cell weight (DCW). DCW was measured after harvesting cells by filtration, washing with 20 mM ammonium bicarbonate, and lyophilization.

2.2 Construction of a recombinant strain

The Ppc-ox strain was transformed with pTCP1299 (Osanai et al., 2015) using a previously described method (Hasunuma et al., 2016) to yield strain Ppc-ox/Δ*ackA*. Colonies resistant to 50 mg/L kanamycin and 34 mg/L chloramphenicol were selected. Knockout of *ackA* (*sll1299*) was confirmed by PCR using the specific primers 5'-TCAGCATTGATACCACTATGGGCTTCAC-3' and 5'-GACAGCCCAGAGACTCCGAGCAAACCGGA-3'.

2.3 Batch fermentation under anaerobic conditions

After pre-cultivation in BG11 medium, cells were inoculated into modified-BG11 medium containing 50 mM Hepes-KOH (pH 7.8) and 5 mM NH_4Cl as a nitrogen

source instead of $NaNO_3$ at a biomass concentration of 0.1 g-DCW/L. Photoautotrophic cultivation proceeded for 3 days under 1% (v/v) CO_2 and continuous light irradiation of 105-115 μmol photons/m^2/s at 30°C as described previously (Hasunuma et al., 2016). After photoautotrophic cultivation, cells were transferred into 100 mM Hepes-KOH (pH 7.8) at biomass concentrations of 5-50 g-DCW/L and cultivated at 30-40°C under anaerobic conditions as described (Hasunuma et al., 2016). Organic acids secreted into fermentation medium were analyzed with high-performance liquid chromatography (HPLC), while minor components were quantified with capillary electrophoresis-mass spectrometry (CE-MS) (CE, Agilent G7100; MS, Agilent G6224AA LC/MSD TOF; Agilent Technologies, Palo Alto, CA, USA) again as described (Hasunuma et al., 2016).

2.4 Analysis of intracellular metabolites

Cells (5 mg DCW) were collected by filtration with 1-μm pore size PTFE disks (Omnipore; Millipore, Billerica, MA,). After washing with 20 mM ammonium carbonate at 4°C, intracellular metabolites were extracted according to previous methods (Hasunuma et al., 2016). To remove solubilized protein, the extract was filtered through a 3 kDa cut-off membrane (Millipore). The metabolites were analyzed using a CE-MS system as described above. Intracellular glycogen was determined with HPLC after extraction from cells and enzymatic hydrolysis (Hasunuma et al., 2016).

2.5 ^{13}C-labeling metabolomics

Metabolite turnover in *Synechocystis* 6803 was determined by the combination of *in vivo* ^{13}C-labeling and CE-MS analysis (Hasunuma et al., 2016). Cells were labeled in 100 mM Hepes-KOH (pH 7.8) containing 2 g/L [U-^{13}C] glucose for 0.5-3 h. After cell collection and metabolite extraction, mass spectra of the intracellular metabolites were analyzed using CE-MS to observe mass shifts from ^{12}C to ^{13}C in metabolites. ^{13}C fractions, ratios of ^{13}C to total carbon, were calculated by relative isotopomer abundance (m_i) of metabolites incorporating i^{13}C atoms as follows:

$$m_i(\%) = \frac{M_i}{\sum_{j=0}^{n} M_j} \times 100$$

$$^{13}\mathrm{C\ fraction}\ (\%) = \sum_{i=1}^{n} \frac{i \times m_i}{n}$$

where M_i represents the isotopomer abundance of metabolite incorporating i^{13}C atoms, and n is the number carbon atoms in the metabolite.

2.6 Enzyme assay

Enzyme assays were performed using cells cultivated for 24 h under dark anoxic condition as described in **Section 2.3**. Activities of PEPC were measured as described previously (Hasunuma et al., 2016). NAD-dependent malate dehydrogenase (MDH) activity was determined as follows. About 50 mg-DCW of cells were collected by centrifugation at 6,000 x g for 10 min at 4°C. After discarding the supernatant and washing with extraction buffer (18 mM KH_2PO_4, 27 mM Na_2HPO_4, 15 mM $MgCl_2$, and 100 μM EDTA, pH 8.0), cells were disrupted in 3 mL of the extraction buffer by sonication. Cell debris was removed by

centrifugation at 20,000 x g for 20 min at 4°C to obtain protein extract as supernatant. MDH assay was performed in 1.5 mL aliquots containing 50 mM Tris-HCl (pH7.5), 200 μM NADH, 0.5 mM oxaloacetate and 250 μL of protein extract. Replicate aliquots without oxaloacetate were used as controls. MDH activity was determined by measuring NADH oxidation as a change in absorbance at 340 nm. Protein content was determined using a BCA assay kit as described previously (Hasunuma et al., 2013).

2.7 qPCR analysis

Synechocystis 6803 cells, cultivated at 30°C and 37°C under anaerobic conditions for 24 h, were harvested by centrifugation at 10,000 × g for 1 min and immediately frozen in liquid nitrogen. Total RNA was extracted from the frozen cells using Fruit-mate for RNA Purification (Takara Bio Inc., Shiga, Japan) and a NucleoSpin RNA kit (Takara Bio Inc.) according to the manufacturer instructions. Complementary DNA was synthesized from 30 ng of total RNA by using a ReverTra Ace qPCR RT Master Mix with gDNA Remover (TOYOBO, Osaka, Japan), and qPCR was performed by using THUNDERBIRD SYBR qPCR Mix (TOYOBO) and Mx qPCR Systems (Agilent Technologies) as previously described (Ho et al., 2017). The qPCR primers used in this study were as follows: for *rnpB*, 5'-GTGGAACCGCTTGAGGAATTTG-3' and 5'-TTTTGACAGCATGCCACTGG-3', for *ppc*, 5'-ACGATGCCAGTGATGTGTTG-3' and 5'-TTCAAACAGGGGCACAATGC-3', and for *mdh*, 5'-AGATTTGATGCTGCCCTTGC-3' and 5'-AGTAAGGCGGCAATTTCAGC-3'. Relative transcript levels were evaluated using the level of the *rnpB* encoding RNA subunit of RNase P as a reference, and then

213 normalized by the levels of each gene at 30°C.

214

215

216 ## 3. Results

217 ### 3.1. Increased temperature enhances secretory production of organic acids

218 in *Synechocystis* cells

219 *Synechocystis* 6803 cells were cultivated under photoautotrophic conditions and
220 transferred to dark and anoxic conditions with an initial cell concentration of 5 g-
221 DCW/L to initiate secretion of organic acids by autofermentation. The
222 autofermentation of *Synechocystis* has been so far performed at only 30ºC
223 (Hasunuma et al., 2016; Ueda et al., 2016). In Fig. 1, effects of temperature on
224 secretory production of organic acids were investigated after 72 h fermentation.
225 Acetate and D-lactate increased with increase in the cultivation temperature. The
226 production of succinate reached a maximum value at 37ºC, which was 162.3 mg/L.
227 Other organic acids, which are secreted as minor products, such as fumarate, 2-
228 ketoglutarate, malate, nicotinate, pyruvate and shikimate increased by elevating
229 temperature from 30 to 37ºC (Supplementary Table 1).

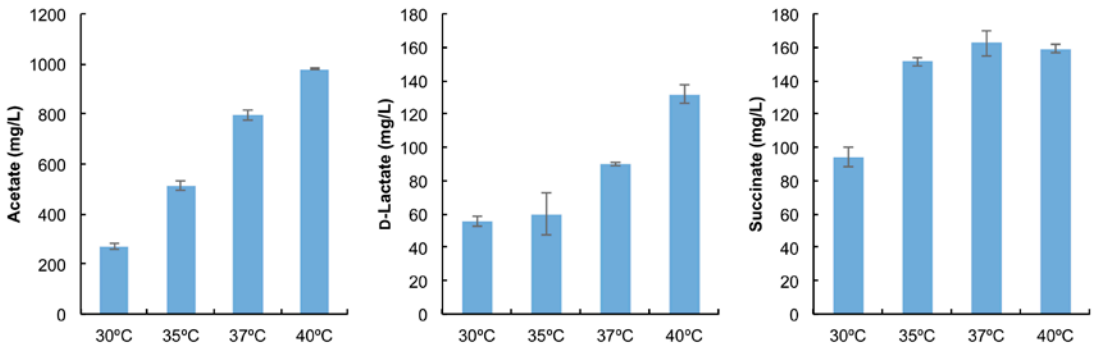

230

231 **Fig. 1** Organic acid produced after 72 h cultivation at various temperatures. Values

represent the average (± SD) of three independent experiments.

In autofermentation, D-lactate and succinate are biosynthesized via sugar catabolism (Hasunuma et al., 2016). The succinate biosynthetic route includes glycolysis, the anaplerotic pathway and the reductive TCA cycle in which PEPC encoded by *ppc* is a rate-limiting enzyme. In fact, overexpression of *ppc* improved succinate production in *Synechocystis* 6803 (Hasunuma et al., 2016). Thus, time-course analysis of organic acid production was carried out using the *ppc*-overexpressing strain, Ppc-ox (Fig. 2). Production of acetate, D-lactate and succinate was enhanced by elevating temperature from 30ºC to 37ºC. Acetate productivity, shown as the slope of Fig. 2, increased together with the increase in temperature. D-lactate production almost reached a plateau after 9 h cultivation at 30ºC, while elevated temperature resulted in a continuous increase in D-lactate even after 9 h of cultivation. Secretion of succinate was initiated after 6 h. The initial slopes of succinate production at 35ºC and 37ºC were higher than that of 30ºC. Ppc-ox exhibited higher production of acetate, D-lactate and succinate at 37ºC, relative to that of the wild-type strain.

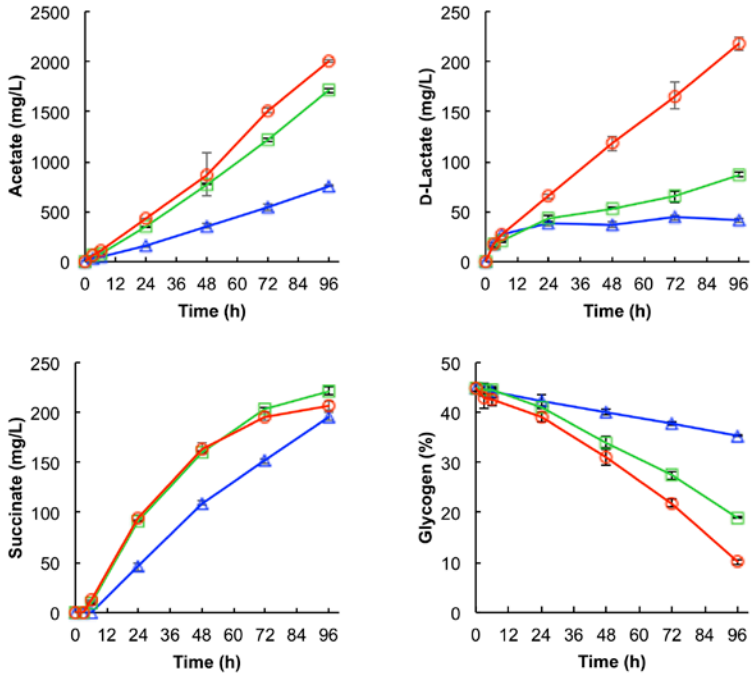

Fig. 2 Time-course of organic acid secreted and intracellular glycogen in Ppc-ox cultivated at 30°C (blue triangles), 35°C (green squares) and 37°C (red circles). Values represent the average (± SD) of three independent experiments.

The time course of intracellular glycogen content in Ppc-ox was compared using three different temperatures (Fig. 2). At 30ºC, glycogen content decreased from 43% to 33%. When the cells were cultivated at 35ºC and 37ºC, glycogen content decreased to 19% and 11%, respectively after 96 h fermentation. Decrease in glycogen at higher temperatures was accompanied by reduction in OD_{750} and less higher density molecules observed with a transmission electron microscope (TEM), while cell number remained constant (Fig. S1).

3.2. The temporal and temperature dependent metabolome

In order to determine the effect of fermentation temperature on dynamic

265 metabolism in Ppc-ox, time course analysis of intracellular metabolites was
266 performed during autofermentation at three different temperatures. Metabolites
267 involved in glycolysis, pentose phosphate pathway (PPP), and TCA cycle, as well as
268 metabolism of amino acids, nucleotides and cofactors, are shown in Fig. 3 and Fig.
269 S2. Accumulation of hexose and pentose phosphates such as glucose 6-phosphate
270 (G6P), fructose 6-phosphate (F6P), fructose 1,6-bisphosphate (FBP), 6-
271 phosphogluconate (6PG), ribulose 5-phosphate (Ru5P), ribose 5-phosphate (R5P)
272 and sedoheptulose 7-phosphate (S7P) was dependent of temperature except for
273 glucose 1-phosphate (G1P). G6P, F6P and FBP continued to increase over time at
274 37°C, while they remained almost constant in the latter half of the fermentation at
275 30°C. The pool size of G1P did not increase after 48 h at 37°C. FBP is converted to
276 glycelaldehyde 3-phophate (GAP) and dihydroxyacetonephosphate (DHAP), which
277 accumulated depending on the temperature. Glycerol 3-phosphate increased along
278 with elevating temperature. The pool size of 3-phosphoglycerate (3PGA), 2-
279 phosphoglycerate (2PGA), and phosphoenolpyruvate (PEP) decreased over time,
280 and this pattern was almost same among the 30°C, 35°C and 37°C groups. Pyruvate,
281 D-lactate and pyruvate-derived amino acids such as alanine, leucine, isoleucine and
282 valine increased dependent on temperature. On the other hand, acetyl-CoA
283 (AcCoA) and metabolites synthesized via the oxidative TCA cycle (including citrate,
284 *cis*-aconitate and isocitrate) decreased with time, and demonstrated lower pool
285 size at higher temperature. Malate, fumarate and succinate synthesized via the
286 reductive TCA cycle demonstrated higher pool size at elevated temperatures until
287 24 h. Arginine, histidine and phenylalanine showed temperature dependent

increases in pool size, while proline decreased with increasing temperature.

The time course of adenosine phosphate and cofactor pool sizes is shown in Fig. 3. Adenylate energy charge, defined as [(ATP) + 1/2 (ADP)] / [(ATP) + (ADP) + (AMP)] (Chapman et al., 1971), decreased along with elevating temperature. Elevated temperature resulted in a slightly lower NAD^+ level than that of 30°C. Reduced NADH and NADPH were not detected with CE-MS due to their low abundance.

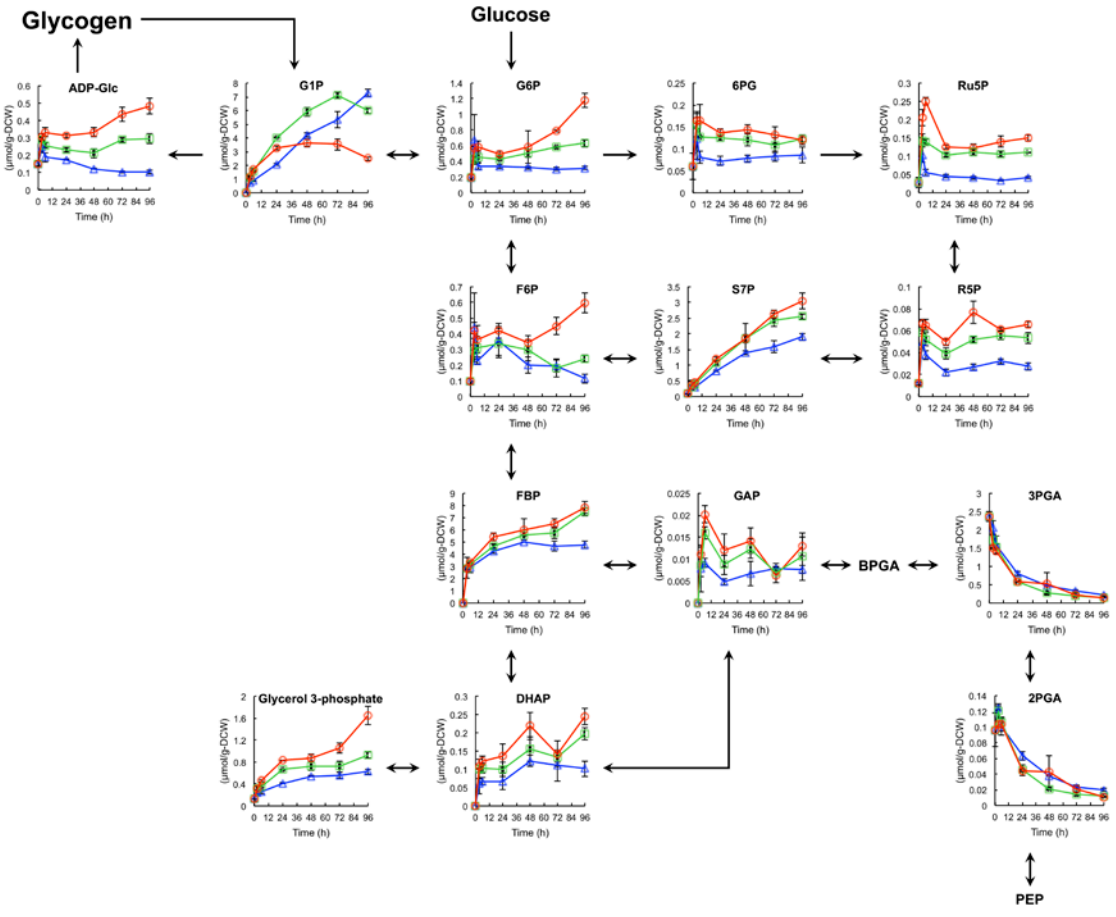

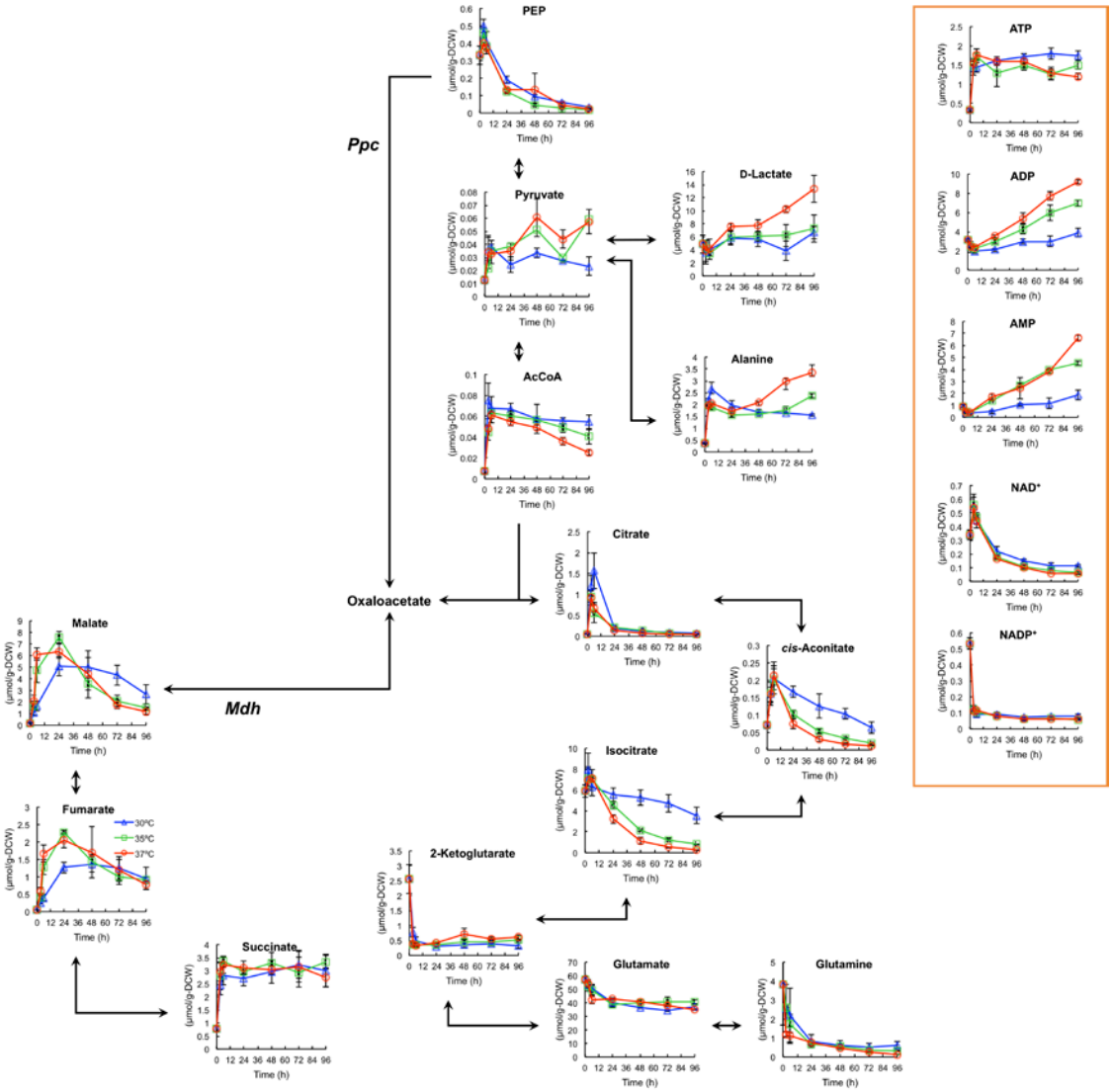

297

298 **Fig. 3** Time course of intracellular metabolite pool size in Ppc-ox cultivated at 30°C
299 (blue triangles), 35°C (green squares) and 37°C (red circles). Abbreviations: AcCoA,
300 acetyl-CoA; ADP-Glc, ADP-glucose; BPGA, 1,3-bisphosphoglycerate; DHAP,
301 dihydroxyacetonephosphate; FBP, fructose 1,6-bisphosphate; F6P, fructose 6-
302 phosphate; GAP, glyceraldehyde 3-phosphate; G1P, glucose 1-phosphate; G6P,
303 glucose 6-phosphate; PEP, phosphoenolpyruvate; 6PG, 6-phosphogluconate; 2PGA,
304 2-phosphoglycerate; 3PGA, 3-phosphoglycerate; R5P, ribose 5-phosphate; Ru5P,
305 ribulose 5-phosphate; S7P, sedoheptulose 7-phosphate. Values represent the average
306 (± SD) of three independent experiments.

3.3. Metabolite turnover under anaerobic conditions reveals a glycolysis to TCA bottleneck

Time course analysis of metabolite pool sizes is insufficient to account for carbon flow and distribution, because the pool size is dependent on the rate of synthesis and utilization of metabolite. Even though a particular reaction is activated under a certain condition, the amount of active metabolite may remain unchanged under steady state conditions.

In the present study, to more comprehensively elucidate the effects of elevating temperature on central metabolism, *in vivo* kinetics of carbon assimilation were investigated using [U-^{13}C] glucose as a tracer compound. Glucose incorporated into the cells is phosphorylated to G6P by glucokinase (Lee et al., 2005), and then metabolized via glycolysis and PPP.

As shown in Fig. 4, metabolites involved in glycolysis and PPP were immediately labeled with ^{13}C after the initiation of the autofermentation. The ^{13}C fraction is defined as the ratio of ^{13}C to total carbon in metabolites, which is obtained by mass spectrometry. Since ADP-glucose, a precursor of glycogen (Fig. 3), and G1P are labeled with ^{13}C, glucose might be utilized to synthesize glycogen. The incorporation of ^{13}C into glycogen was not observed during 3-h ^{13}C labeling, which should be due to the large pool size of glycogen.

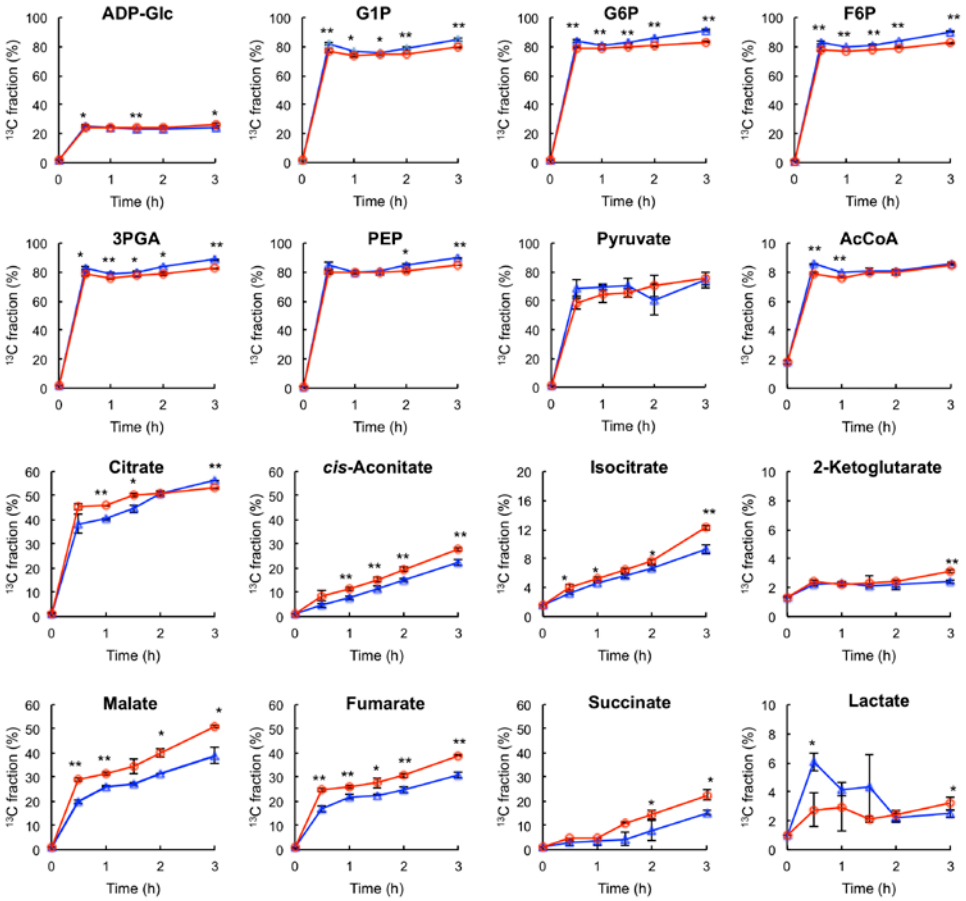

Fig. 4 Time-course changes in ^{13}C fractions of metabolites following ^{13}C-glucose addition to cultures of Ppc-ox cultivated at 30°C (blue triangles) and 37°C (red circles). Values represent the average (± SD) of three independent experiments. Statistical significance was determined using the Student's *t*-test (**P* < 0.05, ***P* < 0.01).

In cyanobacteria, glycogen is hydrolyzed to G1P by glycogen phosphorylase (Aikawa et al., 2015), and then converted to G6P by phosphoglucomutase (Lindahl and Florencio, 2003). Therefore, both G6P derived from glycogen and ^{13}C-G6P derived from [U-^{13}C] can be utilized as carbon sources for organic acids biosynthesis.

Sugar phosphates including G1P, G6P, and F6P and triose phosphates such

as 3PGA demonstrated slightly higher ^{13}C fractions at 30°C relative to that of 37°C, over the course of 3 h fermentation. On the other hand, elevated temperature resulted in significantly higher ^{13}C-fractions of malate, fumarate and succinate when compared to that of 30°C. ^{13}C fractions of pyruvate, lactate, AcCoA, isocitrate and 2-ketoglutarate were similar for both 30°C and 37 °C groups. Increased flux of PEP through the anaplerotic pathway could be clearly observed in the ^{13}C fractions (Fig. S3).

^{13}C enrichment is dependent on the pool size of metabolites. For instance, metabolites whose pool size is large require large amount of ^{13}C to reach high ^{13}C fraction value. Thus, the number of ^{13}C atoms incorporated into metabolites was calculated after 3 h cultivation by multiplying the ^{13}C fraction and pool size (Table 1). Oxaloacetate could not be detected due to its low abundance. With exception to G1P, metabolites involved in glycolysis decreased at 37°C relative to that of 30°C. In contrast, ^{13}C atom numbers of malate, fumarate and succinate increased when elevating temperature from 30°C to 37°C. These results indicate enhanced carbon influx to the reductive TCA cycle. Therefore, the metabolic bottleneck that was previously identified (Hasunuma et al., 2016) had become relaxed. This was accompanied by increases in the specific activity of PEPC and MDH (Fig. 5). mRNA levels of *ppc* and *mdh* increased together with the activity of these enzymes which are involved in the carbon influx (Fig. 6). ^{13}C atom number of D-lactate also increased with elevating temperature.

Table 1 Number of ^{13}C atoms in metabolites.

Metabolite	^{13}C atom number (μmol/g-DCW)	
	30ºC	37ºC
G1P	501.2 ± 15.8	685.2 ± 45.7*
G6P	274.4 ± 27.5	236.6 ± 16.9
F6P	230.8 ± 7.5	194.6 ± 14.9*
3PGA	667.3 ± 63.6	484.0 ± 35.8*
2PGA	47.2 ± 3.1	38.3 ± 4.2*
PEP	200.3 ± 11.7	149.2 ± 9.4**
Pyruvate	7.1 ± 2.6	5.4 ± 1.3
AcCoA	128.6 ± 18.1	84.7 ± 9.5*
Citrate	444.5 ± 61.4	409.8 ± 10.8
cis-Aconitate	14.7 ± 3.5	10.0 ± 0.5
Isocitrate	392.5 ± 58.3	480.6 ± 86.2
2-Ketoglutarate	7.1 ± 1.2	10.0 ± 0.5*
Malate	170.9 ± 33.5	596.7 ± 121.1*
Fumarate	33.2 ± 6.6	115.2 ± 24.4*
Succinate	157.7 ± 26.9	354.9 ± 60.0*
Lactate	31.0 ± 7.2	59.2 ± 11.7*

The number of ^{13}C atoms incorporated into metabolites was measured 3 h after addition of ^{13}C-glucose by multiplying the ^{13}C fraction, pool size and carbon number. Values represent the average (± SD) of three independent experiments. Statistical significance was determined using the Student's *t*-test (*P < 0.05, **P < 0.01).

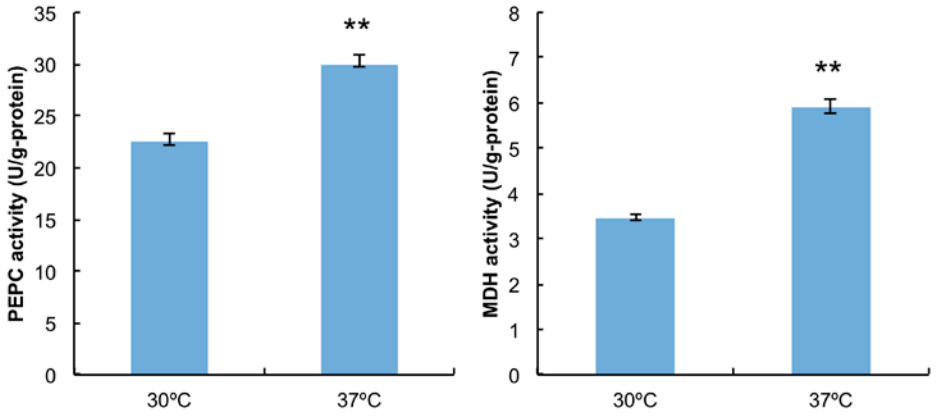

Fig. 5 Phosphoenolpyruvate carboxylase (PEPC) and malate dehydrogenase (MDH) specific activities measured after 24 h fermentation. Values represent the average (± SD) of three independent experiments. Statistical significance was determined using the Student's *t*-test (**P < 0.01).

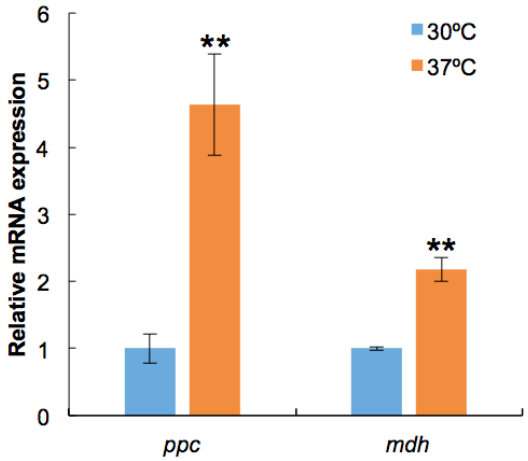

Fig. 6 Relative expression levels of *ppc* and *mdh* at 30°C and 37°C. Relative transcript levels were evaluated using the level of *rnpB* as a reference, and then normalized by the levels of each gene at 30°C. Values represent the average (± SD) of three independent experiments. Statistical significance was determined using the Student's *t*-test (**$P < 0.01$).

In Fig. 4, the initial slope of ^{13}C-fraction indicates turnover of metabolites. Organic acids showed slower turnover than sugar phosphates and triose phosphates at both temperatures. Therefore, a bottleneck is still present at one of the reactions between glycolysis and the TCA cycle in Ppc-ox grown at 37°C.

3.4. Improvement of succinate bioproduction

PEPC forms the TCA intermediate oxaloacetate via reaction of the glycolysis intermediate PEP with bicarbonate. In order to improve succinate production from

the TCA cycle, sodium bicarbonate was added to the fermentation. As shown in Fig. 7, an additive effect of high temperature and $NaHCO_3$ addition on the secretory production of D-lactate and succinate was observed. Succinate production was the highest (400.8 mg/L) in the presence of 100 mM $NaHCO_3$ at 37°C in Ppc-ox. The highest D-lactate (1,097.9 mg/L) titer was obtained in the presence of 200 mM $NaHCO_3$. The addition of up to 300 mM $NaHCO_3$ resulted in increases of pH from 7.6 to no higher than 7.8.

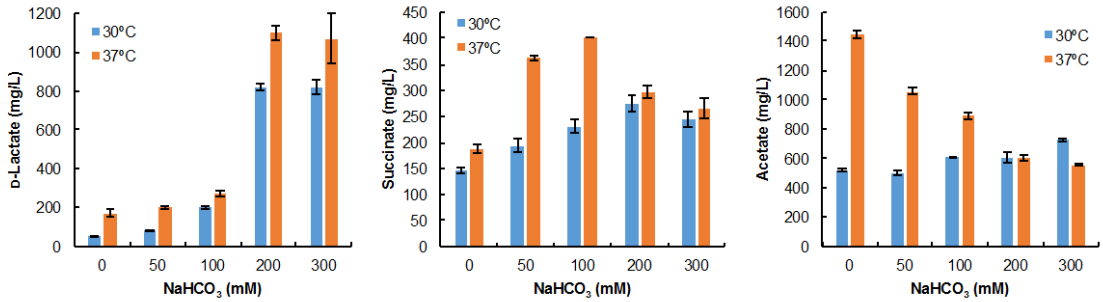

Fig. 7 Effect of $NaHCO_3$ addition on D-lactate, succinate and acetate production after 72 hours fermentation. Bars on the left hand side in blue and bars on the right hand side in orange indicate concentrations at 30°C and 37°C, respectively. Values represent the average (± SD) of three independent experiments.

Effect of initial cell concentration on D-lactate and succinate production was also investigated at 37°C in the presence of 100 mM $NaHCO_3$ (Fig. 8). Production of D-lactate and succinate was dependent on the initial cell concentration, with the highest concentration of D-lactate (1,520.3 mg/L) and succinate (1,802.3 mg/L) produced using 25 g-DCW/L (Fig. 8). Both succinate and lactate titers stopped improving after the initial cell concentration was increased to

413 over 25 g-DCW/L.

414 Since acetate was a major byproduct during succinate production, further
415 optimization of succinate and lactate production was investigated by knocking out
416 the acetate kinase (AK) gene (*ackA*, sll1299) in the Ppc-ox strain. This resulted in
417 significantly lower production of acetate byproduct, while D-lactate production
418 increased to 10.7 g/L, the highest reported titer in cyanobacteria (Fig. 8, lower
419 panels). Although succinate production in Ppc-ox/Δ*ackA* decreased when using cell
420 densities of 25 and 37.5 g-DCW/L, succinate levels slightly increased when using 5,
421 12.5 and 50 g-DCW/L. Interestingly, without *ackA*, levels of PEP, pyruvate and
422 AcCoA all increased which is consistent with higher lactate production (Fig. 9).
423 Despite the increases in lactate and succinate production, knockout of *ackA* did not
424 affect culture pH. This may be due to the presence of 100 mM Hepes-KOH, pH 7.8,
425 or by the additional $NaHCO_3$ during increased lactate production.
426
427

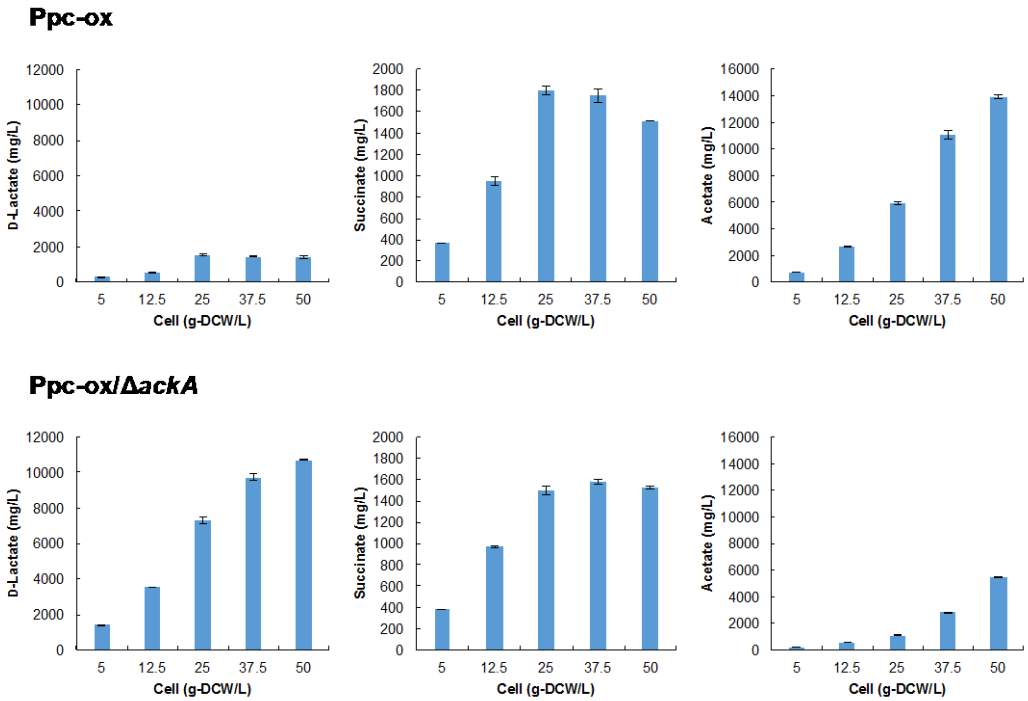

Fig. 8 D-lactate, succinate and acetate produced after 72 hours fermentation at 37°C using 100 mM $NaHCO_3$ and various initial cell concentrations. Organic acid production in the Ppc-ox strain is shown in the upper 3 panels, and production in the *ackA* knockout of Ppc-ox is shown in the lower 3 panels. Values represent the average (± SD) of three independent experiments.

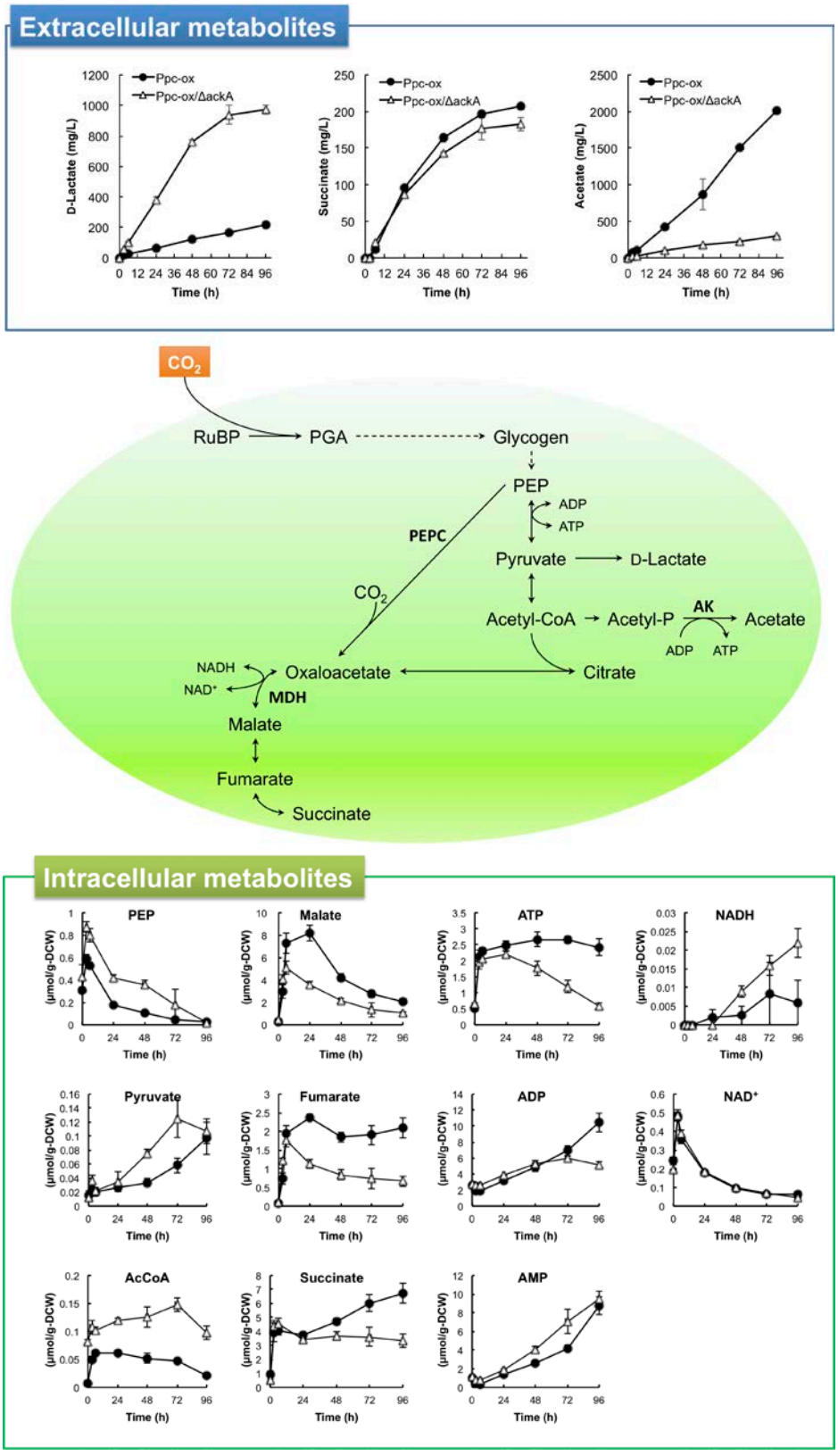

435

436

437 **Fig. 9** Time-course of organic acid secretion and intracellular metabolites in Ppc-ox

438 (closed circles, also shown in Fig. 2) and Ppc-ox/Δ*ackA* (open triangles) cultivated

anaerobically at 37ºC without $NaHCO_3$ supplementation. Values represent the average (± SD) of three independent experiments. Effects of *ackA* deletion on organic acid production are shown in the upper panel, and effects on related intracellular metabolites are shown in the lower two panels. The middle panel shows the pathway to succinate discussed in this study.

4. Discussion

In this study, temperature enhanced secretory production of organic acids in *Synechocystis* 6803 was observed under dark anoxic conditions. A metabolomics approach unveiled dynamic variations in the pool size and turnover of metabolites dependent on the fermentation temperature. To the best of our knowledge, this is the first comprehensive temperature dependent metabolomics study of a microorganism (Yurkovich et al., 2017).

Analysis of ^{13}C-fraction turnover indicates that a bottleneck between PEP and the TCA cycle was relaxed by increasing temperature from 30ºC to 37ºC (Fig. 4). The pool size of citrate, *cis*-aconitate and isocitrate was lower at 37ºC, while malate, fumarate and succinate were increased by elevating temperature during 24 h fermentation (Fig. 3). ^{13}C atom number of malate, fumarate and succinate greatly increased with elevating temperature (Table 1). The TCA cycle in *Synechocystis* 6803 is branched into oxidative and reductive routes. These results suggest that increase in temperature boosts the reductive TCA cycle to produce succinate.

A few studies have reported effects of temperature on bioproduction. For example, production of succinate in *E. coli* strain SBS550MG was not significantly

affected by temperatures of 37°C or 43°C, whereas glucose concentration, CO_2 concentration, pH and cell density were all found to be important factors (Martínez et al., 2011). For production of ascorbic acid-2-phosphate in *Brevundimonas diminuta*, cell density, pH and temperature were key variables, with an optimal temperature of 40°C (Shin et al., 2007). Increase in temperature from 33 to 39.5°C was found to induce glutamate production in *Corynebacterium glutamicum* (Gourdon and Lindley, 1999). However, the metabolic pathways underlying the effects of temperature increase on bioproduction have not been comprehensively investigated.

In the current study, glycogen was produced during photosynthesis, followed by utilization of glycogen and carbon dioxide as carbon sources. Overexpression of *ppc* increased glycogen utilization to 89% and also improved succinate production at 37°C. Throughout fermentation cell density remained constant while OD_{750} and TEM observed high density particles both decreased, indicating the consumption of glycogen (Fig. S1). Although the optimal temperature of *Synechocystis* 6803 PEPC was reported to be 30°C, the enzyme retained 80% of its activity at 40°C and was tolerant to allosteric inhibition (Takeya et al., 2017).

Global transcriptional analysis of *E. coli* indicates that a decrease in temperature from 37°C to 28°C results in an increase in TCA cycle encoding enzymes (Gadgil et al., 2005). Conversely, a 30°C to 45°C temperature increase led to increased glycolytic flux, decreased flux from the TCA cycle into anabolic pathways, and a decrease in adenylate energy charge (Wittmann et al., 2007).

AMP and ADP allosterically activate the *E. coli* glycolytic enzymes pyruvate kinase II (Kotlarz et al., 1975) and phosphofructokinase I (Babul, 1978), respectively (Li et al., 2017). Additionally, oxidative phosphorylation generates ATP from NADH, which inhibits *E. coli* citric acid enzymes pyruvate dehydrogenase (Kim et al., 2008) and citrate synthase (Talgoy and Duckworth, 1979; Weitzman, 1981). Thus, higher concentrations of ATP slow down central metabolism (Kihira et al., 2011), and a 10% decrease in ATP concentration was enough to exert a beneficial effect on succinate production (Li et al., 2017). Reduction of anaerobic ATP levels via PEP synthase mediated futile cycling was also critical to obtain the impressive heterotrophic succinate titer of 31.87 g/L (Li et al., 2017). Accordingly, in the current study, increasing temperature to 37°C had a dramatic effect on the increase of ADP and AMP concentrations, and a moderate but significant effect on lowering ATP level. Therefore, the current study further emphasizes that lowering adenylate energy charge is an effective strategy for increasing autotrophic succinate yields.

Reducing anaerobic NADH/NAD^+ ratio by overexpression of the fumarate reductase gene was reported to be important for increasing succinate yield in *E. coli* (Li et al., 2017). A high NADH/NAD^+ ratio has also been reported to have a negative effect on bioproducton of glutamate in *C. glutamicum* (Gourdon and Lindley, 1999). Conversely, in the cyanobacteria *Synechococcus* sp. PCC 7002, knockout of nitrate reductase led to an increase in NADH/NAD^+ ratio as well as glycogen, H_2, lactate and glycogen production (Qian et al., 2016). Cyanobacteria nitrogen reduction normally leads to NADH consumption and catabolism of

509 glycogen via glycogen phosphorylase and phosphoglucomutase. Accordingly,
510 glycogen metabolism and NADH/NAD^+ ratio should be carefully investigated and to
511 further optimize the autotrophic production of succinate.

512 Under anaerobic conditions cyanobacteria run their TCA cycle backwards
513 from oxaloacetate to succinate (Fig. 9), which generates NAD^+ from NADH. In this
514 study, overexpression of *ppc* in the metabolically engineered strain Ppc-ox provides
515 more oxaloacetate for this route. Additional *ackA* knockout in Ppc-ox results in
516 increased levels of glycolytic intermediates PEP, pyruvate and AcCoA, while TCA
517 intermediates to succinate decreased (Fig. 9). This indicates that in the Ppc-ox *ackA*
518 knockout PEPC can no longer overcome the glycolysis to TCA bottleneck mentioned
519 above, and therefore additional overexpression of the pyruvate carboxylase (PC)
520 gene may be useful to further increase succinate titers (Meng et al., 2016). As
521 NADH levels also increase in the Ppc-ox *ackA* knockout, the overexpression of
522 malate dehydrogenase or NADH dependent fumarate reductase genes are
523 additional options to improve succinate production while at the same time
524 decreasing NADH/NAD^+ ratio (Li et al., 2017).

525 Previous knockout of *ackA* together with overexpression of *SigE* and 200
526 mM KCl supplementation in *Synechococcus* 6803 resulted in an increase of
527 succinate titers up to 141 mg/L and an increase of lactate titers up to 217.6 mg/L
528 (Table 2, Ueda et al., 2016). In the current report, knockout of *ackA* further
529 improved succinate titers over 10 fold using *Synechocystis* 6803 Ppc-ox. Although
530 impressive succinate titers have been achieved using heterotrophic *E. coli* grown
531 with glucose as an energy source (Li et al., 2017), production in autotrophic cells

must be optimized in order to develop a renewable process. Cyanobacteria succinate production has previously been optimized using a variety of strategies (Table 2). Using only photosynthetic conditions, succinate levels could be increased further in *Synechococcus elongatus* PCC 7942 to 430 mg/L (Lan et al., 2016). In the current autotrophic study, the highest autotrophic succinate titer of 1.8 g/L was achieved using the metabolically engineered strain Ppc-ox with overexpression of *ppc* in combination with a straightforward approach of carbon dioxide utilization, and elevation of fermentation temperatures to 37°C.

Table 2 Comparison of cyanobacteria succinate bioproduction studies.

Study	Organism	Conditions	Succinate Titer (Cultivation time)	Succinate Productivity (Cultivation time used for calculation)
Li et al., 2016	*Synechococcus elongatus* PCC 7942	Photosynthetic, nitrogen starvation, *Δglgc, +gltA, +ppc*	435.0 µg/L (48 h)	9 µg/L/h (0-48 h)
Huang et al., 2016	*Synechococcus elongatus* PCC 7942	Photosynthetic, nitrogen starvation, repression of *glgc*, *sdhA*, *sdhB*	580-630 µg/L (48 h)	13 µg/L/h (0-48 h)
Osanai et al., 2015	*Synechococcus* sp. PCC 6803	Dark anaerobic, *+sigE, ΔackA*	~115 mg/L (96 h)	1.38 mg/L/h (0-96 h)
Ueda et al., 2016	*Synechococcus* sp. PCC 6803	Dark anaerobic, *+sigE*, *ΔackA*, 200 mM KCl	141.0 mg/L (72 h)	2 mg/L/h (0-72 h)
Lan et al., 2016	*Synechococcus elongates* PCC 7942	Photosynthetic, overexpression of 4 genes*	430 mg/L (192 h)	3.33 mg/L/h (72-96 h)
This study	*Synechocystis* sp. PCC 6803	Dark anoxic, Ppc-ox, $NaHCO_3$, 37°C	1.8 g/L (72 h)	25 mg/L/h (0-72 h)

*The study by Lan et al. utilized overexpression of α-ketoglutarate decarboxylase,

545 succinate semialdehyde dehydrogenase, citrate synthase and PEPC genes.

546

547

548 **Acknowledgements**

549 The authors thank Ms. Ryoko Yamazaki and Ms. Yui Tamagaki for their technical
550 assistance. This work was supported by Advanced Low Carbon Technology
551 Research and Development Program (ALCA) from the Japan Science and
552 Technology Agency (JST), the Ministry of Education, Culture, Sports, Science, and
553 Technology (MEXT), Japan. This work was also supported by JSPS KAKENHI Grant
554 Number JP15H05557.

555

556

557 **References**

558 Aikawa, S., Ho, S.H., Nakanishi, A., Chang, J.S., Hasunuma, T., Kondo, A. 2015.
559 Improving polyglucan production in cyanobacteria and microalgae via cultivation
560 design and metabolic engineering. Biotechnol. J. 10, 886-898.
561
562 Aikawa, S., Joseph, A., Yamada, R., Izumi, Y., Yamagishi, T., Matsuda, F., Kawai, H.,
563 Chang, J.S., Hasunuma, T., Kondo, A. 2013. Direct conversion of *Spirulina* to ethanol
564 without pretreatment or enzymatic hydrolysis processes. Energy Environ. Sci. 6,
565 1844-1849.
566
567 Akhtar, J., Idris, A., Abd. Aziz, R., 2014. Recent advances in production of succinic
568 acid from lignocellulosic biomass. Appl. Microbiol. Biotechnol. 98, 987-1000.
569
570 Angermayr, S.A., Gorchs Rovira, A., Hellingwerf, K.J., 2015. Metabolic engineering of
571 cyanobacteria for the synthesis of commodity products. Trends Biotechnol. 33,
572 352–361.
573
574 Babul, J., 1978. Phosphofructokinases from *Escherichia coli*. J. Biol. Chem. 253,
575 4350–4355.
576
577 Chapman, A.G., Fall, L., Atkinson, D.E., 1971. Adenylate energy charge in *Escherichia*
578 *coli* during growth and starvation. J. Bacteriol. 108, 1072-1086.
579

Choi, S., Song, C.W., Shin, J.H., Lee, S.Y., 2015. Biorefineries for the production of top building block chemicals and their derivatives. Metab. Eng. 28, 223-239.

Delhomme, C., Weuster-Botz, D., Kühn, F.E., 2009. Succinic acid from renewable resources as a C4 building-block chemical – a review of the catalytic possibilities in aqueous media. Green Chem. 11, 13-26.

Dismukes, G.C., Carrieri, D., Bennette, N., Ananyev, G.M., Posewitz, M.C., 2008. Aquatic phototrophs: efficient alternatives to land-based crops for biofuels. Curr. Opin. Biotechnol. 19, 235–240.

Formighieri, C., Melis, A., 2015. A phycocyanin center dot phellandrene synthase fusion enhances recombinant protein expression and β-phellandrene (monoterpene) hydrocarbons production in *Synechocystis* (cyanobacteria). Metab. Eng. 32, 116–124.

Gadgil, M., Kapur, V., Hu, W.S., 2005. Transcriptional response of *Escherichia coli* to temperature shift. Biotechnol. Prog. 5, 41-44.

Gourdon, P., Lindley, N.D., 1999. Metabolic analysis of glutamate production by *Corynebacterium glutamicum*. Metab. Eng. 1, 224-231.

Hasunuma, T., Matsuda, M., Kondo, A., 2016. Improved sugar-free succinate production by *Synechocystis* sp. PCC 6803 following identification of the limiting steps in glycogen catabolism. Metab. Eng. Commun. 3, 130-141.

Hasunuma, T., Matsuda, M., Senga, Y., Aikawa, S., Toyoshima, M., Shimakawa, G., Miyake, C., Kondo, A., 2014. Overexpression of flv3 improves photosynthesis in the cyanobacterium *Synechocystis* sp. PCC 6803 by enhancement of alternative electron flow. Biotechnol. Biofuel. 7, 493.

Ho, S.H., Nakanishi, A., Kato, Y., Yamasaki, H., Chang, J.S., Misawa, N., Hirose, Y., Minagawa, J., Hasunuma, T., Kondo, A., 2017. Dynamic metabolic profiling together with transcription analysis reveals salinity-induced starch-to-lipid biosynthesis in alga *Chlamydomonas* sp. JSC4, Sci. Rep. 7: 45471.

Huang, C.H., Shen, C.R., Li, H., Sung, L.Y., Wu, M.Y., Hu, Y.C., 2016. CRISPR interference (CRISPRi) for gene regulation and succinate production in cyanobacterium *S. elongatus* PCC 7942. Microb. Cell Fact. 15, 196.

Iijima, H., Nakaya, Y., Kuwahara, A., Hirai, M.Y., Osanai, T., 2015. Seawater cultivation of freshwater cyanobacterium *Synechocystis* sp. PCC 6803 drastically alters amino acid composition and glycogen metabolism. Front. Microbiol. 6, 326.

Ikada, Y., Jamshidi, K., Tsuji, H., Hyon, S.H., 1987. Stereocomplex formation between enantiomeric poly (lactides). Macromolecules 20, 904–906.

Kaneko, T., Sato, S., Kotani, H., Tanaka, A., Asamizu, E., Nakamura, Y., Miyajima, N., Hirosawa, M., Sugiura, M., Sasamoto, S., Kimura, T., Hosouchi, T., Matsuno, A., Muraki, A., Nakazaki, N., Naruo, K., Okumura, S., Shimpo, S., Takeuchi, C., Wada, T., Watanabe, A., Yamada, M., Yasuda, M., Tabata, S., 1996. Sequence analysis of the genome of the unicellular cyanobacterium *Synechocystis* sp. strain PCC 6803. II. Sequence determination of the entire genome and assignment of potential protein-coding region. DNA Res. 3, 109–136.

Kihira, C., Hayashi, Y., Azuma, N., Noda, S., Maeda, S., Fukiya, S., Wada, M., Matsushita, K., Yokota, A. 2012. Alterations of glucose metabolism in *Escherichia coli* mutants defective in respiratory-chain enzymes. J. Bacteriol. 158, 215-223.

Kim, Y., Ingram, L.O., Shanmugam, K.T., 2008. Dihydrolipoamide dehydrogenase mutation alters the NADH sensitivity of pyruvate dehydrogenase complex of *Escherichia coli* K-12. J. Bacteriol. 190, 3851–3858.

Kotlarz, D., Garreau, H., Buc, H., 1975. Regulation of the amount and of the activity of phosphofructokinases and pyruvate kinases in *Escherichia coli*. Biochim. Biophys. Acta. 381, 257–268.

Lai, M.C., Lan, E.I., 2015. Advances in metabolic engineering of cyanobacteria for photosynthetic biochemical production. Metabolites 5, 636–658.

Lan, E.I., Wei, C.T., 2016. Metabolic engineering of cyanobacteria for the photosynthetic production of succinate. Metab. Eng. 38, 483-493.

Lee, J.M., Ryu, J.Y., Kim, H.H., Choi, S.B., de Marsac, N.T., Park, Y.I., 2005. Identification of a glucokinase that generates a major glucose phosphorylation activity in the cyanobacterium *Synechocystis* sp. PCC 6803. Mol. Cells 19, 256-261.

Li, J., Li, Y., Cui, Z., Liang, Q., Qi, Q., 2017. Enhancement of succinate yield by manipulating NADH/NAD^+ ratio and ATP generation. Appl. Microbiol. Biotechnol. 101, 3153-3161.

Li, H., Shen, C.R., Huang, C.H., Sung, L.Y., Wu, M.Y., Hu, Y.C., 2016. CRISPR-Cas9 for the genome engineering of cyanobacteria and succinate production. Metab. Eng. 38, 293-302.

Lindahl, M., Florencio, F.J., 2003. Thioredoxin-linked processes in cyanobacteria are as numerous as in chloroplasts, but targets are different. Proc. Natl. Acad. Sci. U.S.A. 100, 16107-16112.

Martínez, I., Lee, A., Bennett, G.N., San, K.Y., 2011. Culture conditions' impact on succinate production by a high succinate producing *Escherichia coli* strain. Biotechnol. Prog. 27, 1225-1231.

Meng, J., Wang, B., Liu, D., Chen, T., Wang, Z., Zhao, X., 2016. High-yield anaerobic succinate production by strategically regulating multiple metabolic pathways based on stoichiometric maximum in *Escherichia coli*. Microb. Cell. Fact. 15, 141.

McNeely, K., Xu, Y., Bennette, N., Bryant, D.A., Dismukes, G.C., 2010. Redirecting reductant flux into hydrogen production via metabolic engineering of fermentative carbon metabolism in a Cyanobacterium. Appl. Environ. Microbiol. 76, 5032-5038.

Osanai, T., Shirai, T., Iijima, H., Nakaya, Y., Okamoto, M., Kondo, A., Hirai, M.Y., 2015. Genetic manipulation of a metabolic enzyme and a transcriptional regulator increasing succinate excretion from unicellular cyanobacterium. Front. Microbiol. 6, 1064.

Qian, X., Kim, M.K., Kumaraswamy, G.K., Agarwal, A., Lun, D.S., Dismukes, G.C., 2016. Inactivation of nitrate reductase alters metabolic branching of carbohydrate fermentation in the cyanobacterium *Synechococcus* sp. strain PCC 7002. Biotechnol. Bioeng. 113, 979-988.

Shin, W.J., Kim, B.Y., Bang, W.G., 2007. Optimization of ascorbic acid-2-phosphate production from ascorbic acid using resting cell of *Brevundimonas diminuta*. J. Microbiol. Biotechnol. 17, 769-773.

Takeya, M., Hirai, M.Y., Osanai, T., 2017. Allosteric inhibition of phosphoenolpyruvate carboxylases is determined by a single amino acid residue in cyanobacteria. Sci. Rep. 7, 41080.

Talgoy, M.M., Duckworth, H.W., 1979. The interactions of adenylates with allosteric citrate synthase. Can. J. Biochem. 57, 385-395.

Tasaka, Y., Gombos, Z., Nishiyama, Y., Mohanty, P., Ohba, T., Ohki, K., Murata, N., 1996. Targeted mutagenesis of acyl-lipid desaturases in *Synechocystis*: evidence for the important roles of polyunsaturated membrane lipids in growth, respiration and photosynthesis. EMBO J. 15, 6416-6425.

Rippka, R., Deruelles, J., Waterbury, J.B., Herdman, M., Stanier, R.Y., 1979. Generic assignments, strains histories and properties of pure culture of cyanobacteria. J. Gen. Microbiol. 111, 1–61.

Shin, W.J., Kim, B.Y., Bang, W.G., 2007. Optimization of ascorbic acid-2-phosphate production from ascorbic acid using resting cell of *Brevundimonas diminuta*. J. Microbiol. Biotechnol. 17, 769-773.

Ueda, S., Kawamura, Y., Iijima, H., Nakajima, M., Shirai, T., Okamoto, M., Kondo, A., Hirai, M.Y., Osanai, T., 2016. Anionic metabolite biosynthesis enhanced by potassium under dark, anaerobic conditions in cyanobacteria. Sci. Rep. 6, 32354.

Wang, Y., Sun, T., Gao, X., Shi, M., Wu, L., Chen, L., Zhang, W., 2016. Biosynthesis of platform chemical 3-hydroxypropionic acid (3-HP) directly from CO_2 in cyanobacterium *Synechocystis* sp. PCC 6803. Metab. Eng. 34, 60–70.

Wee, Y.J., Kim, J.N., Ryu, H.W., 2006. Biotechnological production of lactic acid and its recent applications. Food Technol. Biotechnol. 44, 163–172.

Weitzman, P.D.J., 1981. Unity and diversity in some bacterial citric acid-cycle enzymes. Adv. Microb. Physiol. 22, 185–244.

Wijffels, R.H., Kruse, O., Hellingwerf, K.J., 2013. Potential of industrial biotechnology with cyanobacteria and eukaryotic microalgae. Curr. Opin. Biotechnol. 24, 405–413.

Williams, J.G.K., 1988. Construction of specific mutations in photosystem II photosynthetic reaction center by genetic engineering methods in *Synechocystis* 6803. Methods Enzymol. 167, 766–778.

Wittmann, C., Weber, J., Betiku, E., Krömer, J., Böhm, D., Rinas, U., 2007. Response of fluxome and metabolome to temperature-induced recombinant protein synthesis in *Escherichia coli*. J. Biotechnol. 132, 375-384.

Yurkovich, J.T., Zielinski, D.C., Yang, L., Paglia, G., Rolfsson, O., Sigurjónsson, Ó.E., Broddrick, J.T., Bordbar, A., Wichuk, K., Brynjólfsson, S., Palsson, S., Gudmundsson, S., Palsson, B.O., 2017. Quantitative time-course metabolomics in human red blood cells reveal the temperature dependence of human metabolic networks. J. Biol. Chem. 292, 19556-19564.

Supplementary Materials

Supplementary Table 1 Organic acid produced after 72 h cultivation at 30°C and 37°C. Values represent the average (± SD) of three independent experiments. Statistical significance was determined using the Student's *t*-test (*P < 0.05, **P < 0.01).

Organic acid	Production (mg/L)	
	30ºC	37ºC
Fumarate	11.27 ± 0.74	57.32 ± 8.82*
2-Ketoglutarate	6.75 ± 0.14	13.67 ± 1.65*
Malate	13.38 ± 1.13	46.69 ± 5.11**
Nicotinate	0.07 ± 0.02	0.46 ± 0.03**
Pyruvate	0.64 ± 0.04	1.68 ± 0.16**
Shikimate	0.07 ± 0.01	0.14 ± 0.04

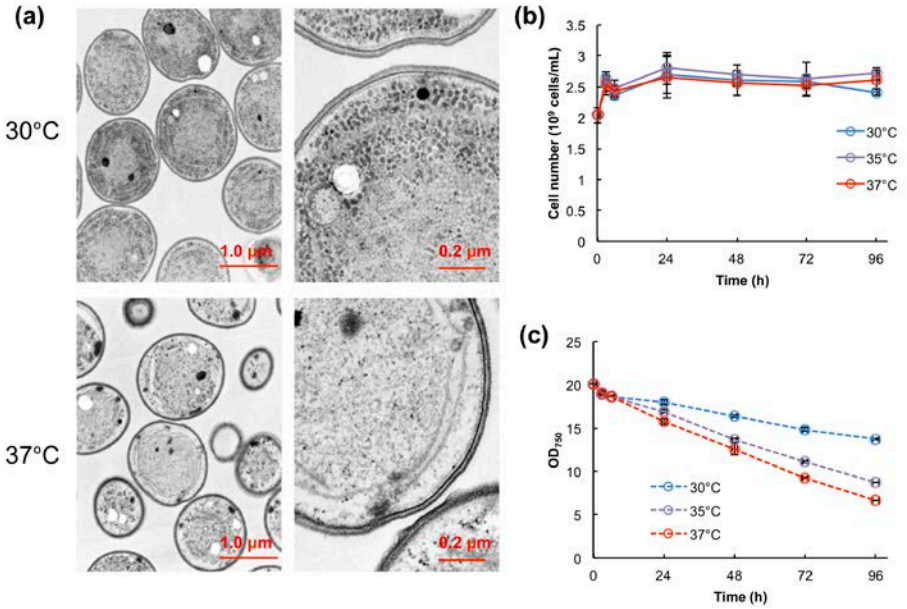

Fig. S1 Transmission electron micrographs of Ppc-ox cultivated at 30ºC and 37ºC for 96 h (a). (b) Time course of cell number at 30ºC (blue circles), 35ºC (purple circles) and 37ºC (red circles). Values represent the average (± SD) of three independent experiments. (c) Decrease in OD_{750} of cells grown at 30ºC (blue circles), 35ºC (purple circles) and 37ºC (red circles). Values represent the average (± SD) of three independent experiments.

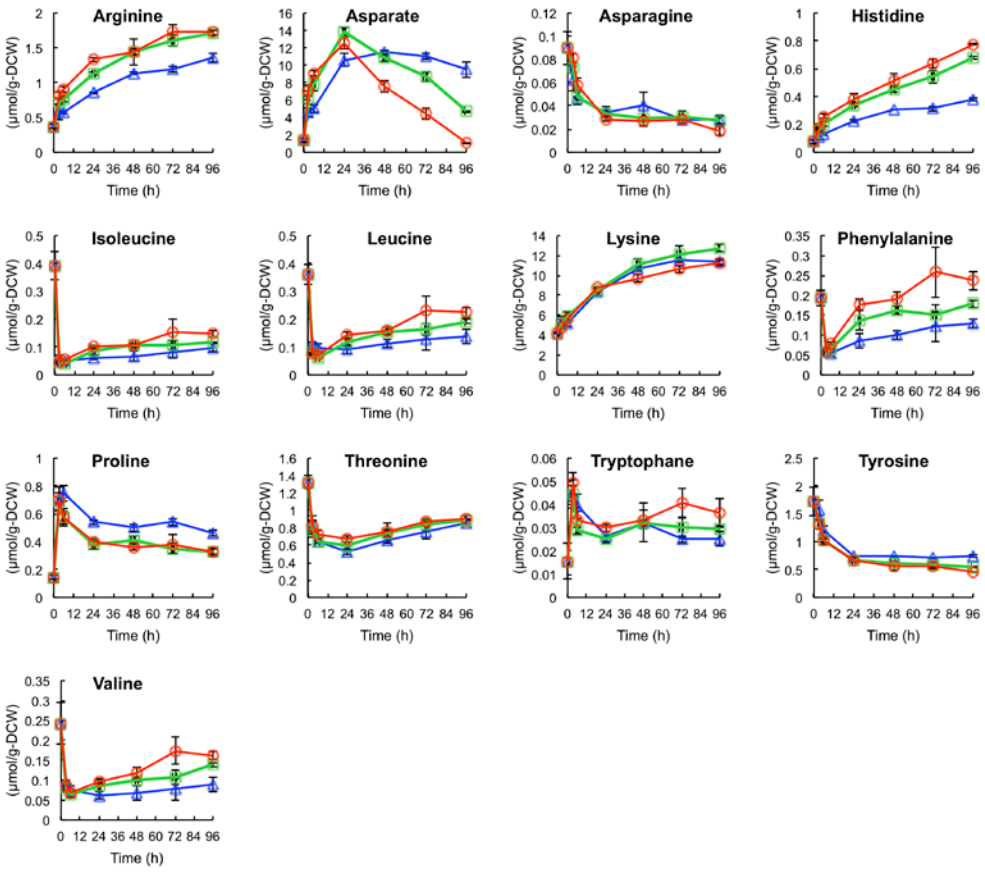

Fig. S2 Time course of intracellular amino acid pool size in Ppc-ox cultivated at 30ºC (blue triangles), 35ºC (green squares) and 37ºC (red circles). Values represent the average (± SD) of three independent experiments.

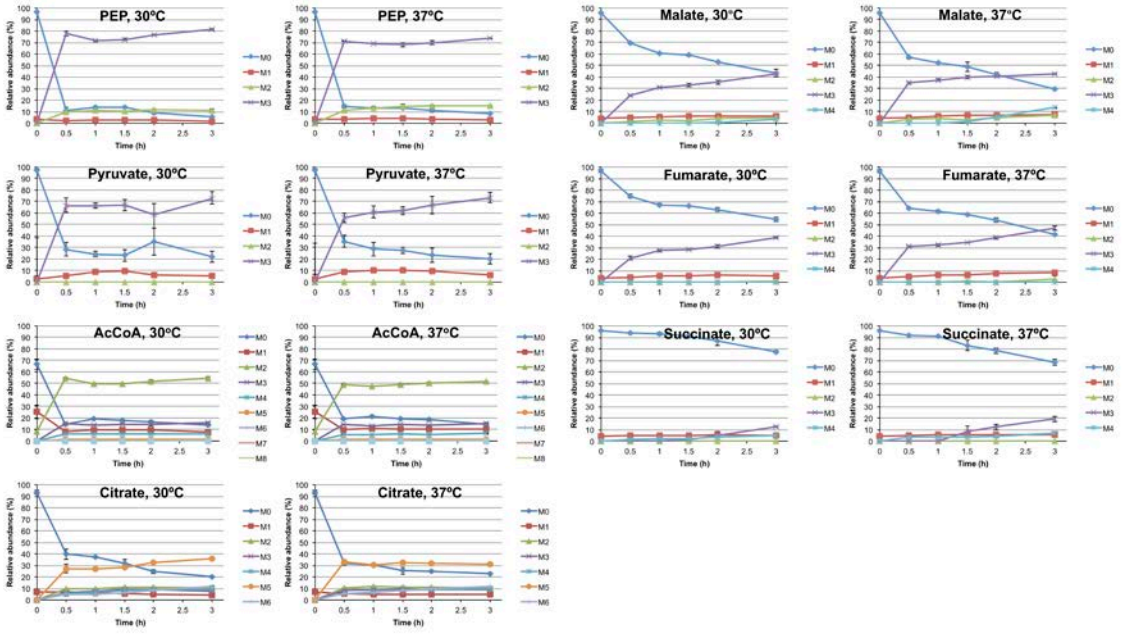

767

768 **Fig. S3** Time-course for mass distribution of metabolites near the pyruvate
769 branch at 30°C and 37°C. Values are the average (± SD) of three independent
770 experiments. Mi represents the relative isotopomer abundance for each metabolite in
771 which *i*^{13}C atoms are incorporated.